

W. HUISINGA<sup>† ‡</sup>, CH. BEST<sup>† §</sup>, R. ROITZSCH<sup>†</sup>,  
CH. SCHÜTTE<sup>†</sup>, AND F. CORDES<sup>†</sup>

## From Simulation Data to Conformational Ensembles: Structure and Dynamics based Methods

---

<sup>†</sup>Konrad-Zuse-Zentrum für Informationstechnik Berlin (ZIB), Germany. Internet:  
<http://www.zib.de/MDgroup>, e-mail: name@zib.de

<sup>‡</sup>supported by the Deutsche Forschungsgemeinschaft (DFG) Schwerpunkt “Ergoden-  
theorie, Analysis und effiziente Simulation dynamischer Systeme” under Grant De 293

<sup>§</sup>Forschungszentrum Jülich (NIC), Germany



# From Simulation Data to Conformational Ensembles: Structure and Dynamics based Methods

W. Huisinga<sup>1 2</sup>, Ch. Best<sup>1 3</sup>, R. Roitzsch<sup>1</sup>, Ch. Schütte<sup>1</sup>, and F. Cordes<sup>1</sup>

## Abstract

Statistical methods for analyzing large data sets of molecular configurations within the chemical concept of molecular conformations are described. The strategies are based on dependencies between configurations of a molecular ensemble; the article concentrates on dependencies induced by a) correlations between the molecular degrees of freedom, b) geometrical similarities of configurations, and c) dynamical relations between subsets of configurations. The statistical technique realizing aspect a) is based on an approach suggested by AMADEI ET AL. (Proteins, 17 (1993)). It allows to identify essential degrees of freedom of a molecular system and is extended in order to determine single configurations as representatives for the crucial features related to these essential degrees of freedom. Aspects b) and c) are based on statistical cluster methods. They lead to a decomposition of the available simulation data into *conformational ensembles* or *subsets* with the property that all configurations in one of these subsets share a common chemical property. In contrast to the restriction to single representative conformations, conformational ensembles include information about, e.g., structural flexibility or dynamical connectivity.

The conceptual similarities and differences of the three approaches are discussed in detail and are illustrated by application to simulation data originating from a hybrid Monte Carlo sampling of a triribonucleotide.

**Key words.** conformational ensemble, cluster method, structural and dynamical similarity, representative, conformation, essential degrees of freedom, transition states, cluster analysis, feature extraction.

**Mathematics subject classification.** 65U05, 62H30.

## 1 Introduction

A molecule can exist in an infinite number of spatial states, in the literature also known as configurations. Subsets of states can be identified as *confor-*

---

<sup>1</sup>Konrad-Zuse-Zentrum für Informationstechnik Berlin (ZIB), Germany. Internet: <http://www.zib.de/MDgroup>, e-mail: [name@zib.de](mailto:name@zib.de)

<sup>2</sup>supported by the Deutsche Forschungsgemeinschaft (DFG) Schwerpunkt "Ergodentheorie, Analysis und effiziente Simulation dynamischer Systeme" under Grant De 293

<sup>3</sup>Forschungszentrum Jülich (NIC), Germany

*mational ensembles*, if all states within the subset share a common chemical property. However, often just a single state is referred to as a conformation, being a typical representative of the chemical property. In this article, we consider both aspects with the main emphasis lying on the ensemble aspect of conformations.

Structurally meta-stable conformations belong to minima of the free energy landscape, which are expected to be nearly isoenergetic [15]. They could be identified experimentally, if the barriers between the minima enabled lifetimes of the states, which correspond to the time resolution of the experiment. Transitions between these conformations have been investigated theoretically; they can be described by a few collective interdomain motions, which correspond to low energy conformational changes [17, 20]. Functionally active conformations can be characterized by their ability to initiate a process. They need neither to be structurally conserved in every atom position, nor necessarily occupy an energy minimum. Up to now, the lifetime of these conformations is generally below experimental resolution, but within the scope of simulations.

Theoretical investigations of simulation data have contributed to the understanding of, e.g., conformational gating of buried active sites [30], binding of ligands to proteins [19], folding processes of proteins [9, 5] or the initial state of an enzymatic reaction [4]. These insights result from analyzing simulated time series below the nanosecond range, which are assumed to correspond to thermodynamical ensembles of the respective molecular system. Although the simulation data are still not large enough to accurately reproduce configurational entropy or free energy, the classification in terms of conformational subsets may help to understand the structure-function relationship of biomolecules and allows to reduce the complexity without losing relevant information.

Cluster methods are well established in many fields to discover the unknown structure of complex data [2, 23]. In our context these methods can be used to decompose some large set of configuration data into disjoint conformational subsets with the property that configurations from one subset are structurally closer to each other than configurations from different subsets. There are two classes of such *structure based* cluster methods: 1) *Global* methods directly handle the entire set of data; they are known from, e.g., clustering in large graphs via spectral information [22, 8] or from decomposition techniques using multiple-center estimations of phase space distributions [26]. 2) *Sequential* methods handle the data set as a sequence and refine the decomposition iteratively; they are based on, e.g., non-hierarchical neural nets [25] or fuzzy clustering [18]. However, none of the structure based cluster methods takes into account any *dynamical* properties of the molecular system underlying the given set of configurations. That is, these methods do not allow to characterize the meta-stability of the conformational subsets, e.g., their lifetimes or the rate of transitions between them. *Dynamics*

*based* cluster techniques have been developed only recently [28]. Based on additional transition data, the set of configurations is decomposed into conformational subsets with respect to meta-stability minimizing the transition probabilities between them.

In [1], Amadei et al. introduced the so-called essential dynamics techniques tailored to identify *essential degrees of freedom* of molecular systems based on simulation data. We will demonstrate in Sec. 2.1, how this technique can also be used as a tool for conformational analysis. In contrast to the cluster analysis tools discussed above, this approach yields single *representative conformations* rather than conformational subsets or ensembles.

The primary concern of this article is to discuss and compare the structure based and dynamical based conformational subsets. To this end, two different cluster techniques and the representative analysis are considered in detail, at first conceptionally in Sec. 2 and then via application to the triribonucleotide adenylyl(3'-5')cytidyl(3'-5')cytidin (r(ACC)) in vacuum (chosen because of its structural flexibility) in Sec. 3.

The required configuration and transition data were computed by means of a specific hybrid Monte Carlo method with adaptive temperature choice (ATHMC) [12], especially designed to overcome energy barriers. Based on the resulting data we observe some interesting and far-reaching similarities between dynamics and structure based conformational subsets but also significant differences, e.g., situations in which configurations from different meta-stable conformational subsets are clustered together by the structure based method.

## 2 Methods

In classical MD a molecule is modeled by a Hamiltonian function

$$H(q, p) = \frac{1}{2} p^T M^{-1} p + V(q),$$

where  $q = (q_1, \dots, q_{3N})$  and  $p = (p_1, \dots, p_{3N})$  are the corresponding positions and momenta of the atoms,  $M$  the diagonal mass matrix, and  $V$  a differentiable potential. The formal solution with initial state  $q_0 = q(0)$ ,  $p_0 = p(0)$  is given by  $q(t) = q(t; q_0, p_0)$  and  $p(t) = p(t; q_0, p_0)$ .

Most experiments on molecular systems are performed under the conditions of constant temperature and volume. The distribution of the identically prepared systems is described by the stationary *canonical density* associated with the Hamiltonian  $H$

$$f(q, p) = \frac{1}{Z} \exp(-\beta H(q, p)),$$

where  $Z$  denotes the partition sum,  $\beta = 1/k_B T$ , with  $T$  being the system's temperature  $T$  and  $k_B$  Boltzmann's constant. Since  $H$  is separable, the

canonical density decomposes into a product of a position density  $Q(q)$  depending only on  $q$  and a momentum density  $P(p)$  depending only on  $p$ , i.e.,  $f_0(q, p) = Q(q)P(p)$ .

Starting point for the methods presented below is a sampling of the positional part of the canonical density resulting in simulation data  $q^{(1)}, \dots, q^{(S)}$ . When using reweighted hybrid Monte Carlo methods, there is a weighting factor associated to each state  $q^{(k)}$ . To keep notation simple, we assume within this section the weighting factor being the same for all states.

## 2.1 Representative Conformations

Identifying representative conformations is based on a correlation analysis of the molecular degrees of freedom. Analysis of simulation data reveals that it is possible to divide the set of molecular degrees of freedom into two subsets: a subset of only a few “essential” degrees of freedom, in which anharmonic motion occurs that comprises most of the positional fluctuations, and the remaining degrees of freedom, in which the motion has a narrow Gaussian distribution and can be considered as “physically constrained” [1]. This is in contrast to normal mode analysis [21], which is based on the shape of the potential energy function and is restricted to predict only harmonic vibrations. We determine essential degrees of freedom both in the Cartesian coordinate space following AMADEI ET AL. [1] as well as in the space of torsion angles.

**Cartesian coordinates.** Since essential degrees of freedom should only reflect internal fluctuations of the molecule, we first eliminate the overall translational and rotational motion. This is done by a least squares translational and rotational fit of each configuration to an arbitrary chosen reference configuration. The results are fitted simulation data, which, for simplicity, we again denote by  $q^{(1)}, \dots, q^{(S)}$ .

The correlation between atomic motions within the simulation data are expressed by the covariance matrix

$$C = \text{Cov}(q_k, q_n)_{k,n=1,\dots,3N} = \langle (q - \langle q \rangle_Q)(q - \langle q \rangle_Q)^T \rangle_Q,$$

where  $\langle \cdot \rangle_Q$  denotes the ensemble average, i.e.,

$$\langle q \rangle_Q = \int_{\Omega} q Q(q) dq \approx \sum_{s=1}^S q^{(s)} Q(q^{(s)}).$$

Since  $C$  is symmetric, it can always be diagonalized. Let  $U$  denote the matrix, whose columns are the eigenvectors of  $C$ . Then the transformed coordinates  $x = U^T(q - \langle q \rangle_Q)$  are uncorrelated and

$$\Lambda = \text{Cov}(x_k, x_n)_{k,n=1,\dots,3N} = \langle x x^T \rangle_Q$$

for a diagonal matrix  $\Lambda = \text{diag}(\lambda_k)$ . If we choose the eigenvectors to be normalized with respect to the Euclidean norm (or equivalently, the matrix  $U$  to be orthogonal), the eigenvalues are equal to the variance of the transformed coordinates, i.e.,  $\text{Var}(x_k) = \lambda_k$  for all  $k$ .

Due to the last equality, the covariance matrix is connected to the systems constraints in the following way [1]: Transformed coordinates corresponding to zero or nearly zero eigenvalues behave effectively as constraints; they have narrow Gaussian distributions with zero mean and do not contribute significantly to the positional fluctuations. In contrast to that, transformed coordinates corresponding to large eigenvalues represent large positional deviations. Often, only a few coordinates see important fluctuations; these are called essential degrees of freedom. In practice, one has to specify a set of largest eigenvalues of  $C$ , which, often, can only be done heuristically.

**Torsion Angles.** An alternative way to describe conformational changes is based on the set of torsion angles  $\omega_1, \dots, \omega_M$  of the molecular system under consideration. In order to analyze the simulation data in terms of these torsion angles we have to apply statistical methods for circular data [13, 14].

The mean direction  $\mu(\omega_k)$  of the torsion angle  $\omega_k$  and a corresponding circular deviation  $\rho(\omega_k)$  are defined by

$$r(\omega_k) \exp(i\mu(\omega_k)) = \langle \exp(i\omega_k) \rangle_Q \quad \text{and} \quad \rho(\omega_k) = \sqrt{-2 \log(r(\omega_k))}.$$

The value  $r(\omega_k)$  is called the mean resultant length. To apply the analysis from above we choose the following definition of correlation between circular variables<sup>4</sup> [13, 14]

$$\text{Cor}(\omega_k, \omega_m) = \frac{r^2(\omega_k - \omega_m) - r^2(\omega_k + \omega_m)}{\sqrt{(1 - r^2(2\omega_k))(1 - r^2(2\omega_m))}}.$$

and set  $\text{Cov}(\omega_k, \omega_m) = \text{Cor}(\omega_k, \omega_m)\rho(\omega_k)\rho(\omega_m)$ . These definitions allow to apply the technique introduced above for simulation data  $\omega^{(1)}, \dots, \omega^{(S)}$  being converted to torsion angles.

The identification of representative conformations is based on the following idea. According to their distribution, essential degrees of freedom can roughly be divided into two groups: (1) broad Gaussian shaped and (2) multiple peaked compounding of Gaussian like parts. Each Gaussian peak corresponds to a part of the configurational space with relevant weighting factor and might be represented by a configuration associated with the maximum of the Gaussian peak. Thus, configurations associated with a combination of maxima of all essential degrees of freedom correspond to the

---

<sup>4</sup>In contrast to the Cartesian coordinate case, there are different definitions of correlations between circular data (see [24, 13] and references therein).

most different states of the molecular system. In order to eliminate artificial combinations of maxima we associate to each combination a weighting factor being defined as the number of states that are within a predefined Euclidean distance to the maxima combination. We sort with respect to the weighting factors and neglect all combinations with zero weight; the representative conformations are then defined as the states that are closest to the combination of maxima.

## 2.2 Clustering Methods

In this section we present two different concepts to identify essential molecular conformations. Although they are based on different aspects of the simulation data, both methods are grounded on the same idea: They exploit special properties of eigenvectors corresponding to a so-called proximity matrix associated with the system.

In order to introduce the identification methods consider the following setting: Given a set of data  $\{d_1, \dots, d_s\}$ , e.g., single configurations or sets of configurations, and a proximity function  $p(d_i, d_j) \in [0, 1]$  measuring the degree of association between two elements. In the case of the methods presented below, the proximity function measures either structural or dynamical relations. It is  $p(d_i, d_j) \approx 1$  for strongly related data and  $p(d_i, d_j) \approx 0$ , if  $d_i$  and  $d_j$  are only weakly related<sup>5</sup>.

We are interested in decomposing the set of data into disjoint clusters (conformations)  $C_1, \dots, C_c$ , such that each cluster  $C_i$  groups together related elements, while elements of different cluster are mostly unrelated. Let  $p(C_i, C_j)$  denote the proximity between the two clusters  $C_i, C_j$  defined by an appropriate average value of  $p(d, \hat{d})$  for  $d \in C_i$  and  $\hat{d} \in C_j$ . Then we ask for a decomposition into clusters  $C_1, \dots, C_c$ , such that

$$p(C_i, C_i) \approx 1 \quad \text{and} \quad p(C_i, C_j) \approx 0, \quad i \neq j. \quad (1)$$

In order to identify the clusters, both methods use a proximity matrix  $P = (P_{ij})$  based on the proximity function  $p$ . The off-diagonal entries are given by  $p(d_i, d_j)$ , while the diagonal entries are different for either method.

In view of Eq. 1 the clustering problem is equivalent to finding a permutation of the data  $d_1, \dots, d_s$  such that the permuted proximity matrix is *as block-diagonal as possible*, in the sense that the average value over off-blockdiagonal entries is much less than the corresponding blockdiagonal value. Since the problem of finding such a permutation is in practice unsolvable (it is a so-called *NP*-complete problem), the methods presented below pursue (different) heuristics. However, both exploit eigenvectors of the proximity matrix.

---

<sup>5</sup>We do not request symmetry, i.e.,  $p(d_i, d_j) = p(d_j, d_i)$  for all  $i, j$ , for the proximity function.



### 2.2.1 Structure Based Conformations

The structural method aims at classifying configurations according to their structural proximity or similarity. The set of configurations is partitioned into disjoint subsets with the property that two configurations in the same subset are in some sense structurally closer to each other than two configurations in different subsets. In the statistical literature, this problem is known as cluster analysis, i.e., the classification of a set of feature vectors by their intrinsic properties [23, 2, 8].

The measure of structural proximity should be invariant under rotations and translations. We thus choose to describe a configuration  $q$  not by the Cartesian positions of its atoms, but by its intra-molecular distances defining a symmetric  $n \times n$  distance matrix<sup>6</sup>  $D(q) = (D_{ij}(q))$  with

$$D_{ij}(q)^2 = \sum_{k=1}^3 |q_{ik} - q_{jk}|^2, \quad i, j = 1, \dots, N.$$

In the statistical literature, the distance matrix is known as feature vector. Since  $D$  is symmetric, it is sufficient to consider only the  $N(N-1)/2$  different intra-molecular distances. With respect to the number of degrees of freedom, the set of different intra-molecular distances is still overdetermined, which allows to further reduce the distance matrix (see Sec. 3).

The structural distance between two configurations  $q$  and  $\hat{q}$  is defined as the distance of their distance matrices:

$$\text{dist}(q, \hat{q}) = \frac{1}{N(N-1)/2} \left( \sum_{i < j}^N (D_{ij}(q) - D_{ij}(\hat{q}))^2 \right)^{1/2}$$

To transform the structural distance into a proximity, we choose<sup>7</sup> the function

$$p(q, \hat{q}) = \exp \left( -\frac{\text{dist}(q, \hat{q})}{c} \right)$$

with a suitably chosen constant  $c$ , which sets the preferred distance scale of the clusters. Distances much smaller than  $c$  are mapped to nearly complete similarity and will almost always form a cluster, while distances much larger than  $c$  are mapped to nearly complete dissimilarity and will rarely form a

---

<sup>6</sup>For sake of simplicity, we assume the components of a configuration  $q = (q_1, \dots, q_{3N})$  ordered in the way that  $(q_{i1}, q_{i2}, q_{i3})$  represents respectively the  $x, y, z$  positions of the  $i$ th atom.

<sup>7</sup>There are other possible transformations, like e.g.,  $p(q, \hat{q}) = 1 - \text{dist}(q, \hat{q})/c$  or  $p(q, \hat{q}) = 1/(1 + \text{dist}(q, \hat{q})/c)$ . However, our cluster algorithm performs best with the proximity function given above.

cluster. The proximity between two clusters  $C_i$  and  $C_j$  is then defined as

$$p(C_i, C_j) = \sum_{q \in C_i, \hat{q} \in C_j} p(q, \hat{q}). \quad (2)$$

The identification of clusters or conformations is attacked hierarchically by gradually partitioning a cluster  $C$  into two subclusters  $C_+, C_-$ . Its basic idea is due to [10, 11, 22]: Let  $\chi_i$  be +1 if configuration  $q^{(i)}$  belongs to  $C_+$ , and -1 if it belongs to  $C_-$ . Then

$$\begin{aligned} p(C_+, C_-) &= \frac{1}{8} \sum_{i,j=1}^S p(q^{(i)}, q^{(j)}) (\chi_i - \chi_j)^2 \\ &= \frac{1}{4} \sum_{i,j=1}^S p(q^{(i)}, q^{(j)}) \chi_i^2 - \frac{1}{4} \sum_{i,j=1}^S p(q^{(i)}, q^{(j)}) \chi_i \chi_j \\ &= \frac{1}{4} \sum_{\substack{i,j=1 \\ i \neq j}}^S \chi_i p(q^{(i)}, q^{(j)}) \chi_i - \frac{1}{4} \sum_{\substack{i,j=1 \\ i \neq j}}^S \chi_i p(q^{(i)}, q^{(j)}) \chi_j \\ &= \frac{1}{4} \sum_{i,j=1}^S \chi_i P_{ij} \chi_j = \frac{1}{4} (\chi, P\chi), \end{aligned}$$

where  $(\cdot, \cdot)$  denotes the Euclidean inner product and  $P$  the proximity or Laplacian matrix

$$P_{i,j} = \begin{cases} -p(q^{(i)}, q^{(j)}) & , \text{ if } i \neq j \\ \sum_{\substack{k=1 \\ k \neq i}}^S p(q^{(i)}, q^{(k)}) & , \text{ if } i = j \end{cases}$$

The cluster problem is to minimize  $(\chi, P\chi)$  under the constraint that  $\chi_i = \pm 1$  and not all  $\chi_i$  are equal. A similar minimality condition arises in diagonalizing a symmetric matrix: The eigenvector  $X$  corresponding to the lowest eigenvalue of the matrix minimizes  $(X, PX)$  under the constraint that  $X$  is normalized; the eigenvalue is equal to the value attained at the minimum. Higher eigenvectors minimize this quantity under the additional constraint of being orthogonal to all lower eigenvectors.

By construction, the matrix  $P$  has a trivial lowest eigenvalue of zero corresponding to the constant eigenvector  $(1, \dots, 1)$ . The second lowest eigenvector  $X$  then represents a minimum of  $(X, PX)$  where  $X$  is orthogonal to the constant vector, i.e., has vanishing sum. It thus will consist of positive and negative (and possibly zero) entries. This differs from the original constraint only in allowing non-integer (or zero) values. We can consider the second eigenvector as a heuristic approximation to the true solution of

the discrete problem by mapping “continuous” entries  $X_i$  to discrete values  $\chi_i = \pm 1$  using a threshold  $t$ :

$$\chi_i = \begin{cases} -1 & \text{if } X_i < t \\ +1 & \text{if } X_i \geq t \end{cases}$$

The threshold  $t$  is determined as the value at which the proximity  $p(C_+, C_-)$  of the two subclusters is minimized. In this way, the second-lowest eigenvector serves as a heuristic for determining the partitioning that must be considered in the minimization procedure. Instead of all partitions, the algorithm considers only those arising from thresholding the second eigenvector. This splitting procedure is repeated iteratively.

Since the proximity of two clusters, as defined in Eq. 2, is not weighted by the size of the subclusters, it favors splitting off a subcluster containing only a single configuration<sup>8</sup>. One could include a suitable weighting factor in the definition of proximity, but this would destroy the connection to the eigenproblem of the Laplacian matrix, though it is still possible to use such a weighting factor when the threshold  $t$  is determined. However, splitting off single configurations only indicates that these configurations do not cluster very well. We found that after a few of these peripheral splits, there occur central splits that result in subclusters of comparable size.

### 2.2.2 Dynamics Based Conformations

The dynamics based clustering characterizes conformations in terms of meta-stability. The state space is partitioned into disjoint subsets (conformations) with the property that each subset is meta-stable with respect to fluctuations within the canonical ensemble. Consequently, transitions between different subsets are rare events. In the first part, we introduce the dynamics within the ensemble and how to approximate it; in the second part, we present a cluster method to identify meta-stable conformations.

The distribution of molecular systems within the canonical ensemble does not change in time. However, there are fluctuations within the ensemble, since single systems evolve according to the Hamiltonian equation of motion. To capture the internal dynamics, we fix a time  $\tau$  and observe all single system fluctuations after the span  $\tau$ . A subset  $C \subset \Omega$  is called invariant under the dynamics, if all systems being in  $C$  stay there after the time  $\tau$ . By definition, the whole configurational space is invariant. Furthermore, a subset  $C$  is called almost invariant or meta-stable, if most of the systems stay in  $C$  after time  $\tau$ .

In order to introduce the measure of dynamical proximity and therefore making the above characterization more precise we approximate the

---

<sup>8</sup>In this case, there will only be  $S - 1$  terms in (2), as opposed to  $S^2/4$  for a symmetric split.

fluctuations within the canonical ensemble. Based on the simulation data  $q^{(1)}, \dots, q^{(S)}$ , we choose for each configuration  $q^{(k)}$  a momentum  $p^{(k)}$  according to the density  $P$  (see Sec. (2)) and integrate the Hamiltonian system for the time  $\tau$ . This results in new configurations  $\hat{q}^{(k)} = q(\tau; q^{(k)}, p^{(k)})$  and transitions<sup>9</sup>  $q^{(k)} \rightarrow \hat{q}^{(k)}$ .

For two subsets  $C_{\text{from}}, C_{\text{to}}$ , the dynamical proximity  $p_\tau(C_{\text{from}}, C_{\text{to}})$  measures the relative frequency of transitions from  $C_{\text{from}}$  to  $C_{\text{to}}$ :

$$p_\tau(C_{\text{from}}, C_{\text{to}}) = \frac{\text{no.}(q^{(k)} \in C_{\text{from}} \text{ and } \hat{q}^{(k)} \in C_{\text{to}})}{\text{no.}(q^{(k)} \in C_{\text{from}})}; \quad (3)$$

it can be interpreted as the conditional transition probability of being in  $C_{\text{from}}$  and changing to  $C_{\text{to}}$  within the time  $\tau$ . We call a subset or conformation  $C$  meta-stable, if  $p_\tau(C, C) \approx 1$  and a transition a rare event, if  $p_\tau(C_{\text{from}}, C_{\text{to}}) \approx 0$ . In contrast to the structure based method, the proximity is defined for subsets of states rather than for single states. To solve the dynamics based cluster problem, i.e., to identify meta-stable conformations, we therefore discretize the state space into disjoint sets  $B_1, \dots, B_d$ , e.g., boxes resulting from a grid defined by partitioning the Cartesian coordinates or torsion angles into intervals, and seek out cluster that can be written in terms of these sets  $B_i$ . At this point, we are in the situation of the general cluster problem presented in Sec. 2.2. Thus, in principle, every cluster algorithm based on the discretization sets  $B_1, \dots, B_d$  and the transition probabilities  $p_\tau(B_i, B_j)$  could be applied to identify meta-stable conformations. In the following we present a cluster method that exploits the special structure of the transition probabilities and can be interpreted as the discretization of a continuous cluster problem (for details, see [28]).

As for the structural method, the identification algorithm is based on a proximity or transition matrix  $P = (P_{ij})$ , which is defined by the transition probabilities,  $P_{ij} = p_\tau(B_i, B_j)$ . For the identification process, we exploit the following two properties of the transition matrix (for more details see [7]):

1. The transition matrix is stochastic, i.e., its entries are non-negative and the sum of each row equals one. As a consequence, the constant vector  $(1, \dots, 1)$  is an eigenvector corresponding to the eigenvalue  $\lambda_1 = 1$ .
2. The presence of meta-stable conformations corresponds to a block structure of the transition matrix (for a suitable permutation of the  $B_i$ ) and a splitting of the spectrum into a cluster of eigenvalues  $\lambda_1, \dots, \lambda_c$  near 1 and the remaining part of the spectrum. The two spectral parts are separated by a gap. The number of meta-stable conformations, blocks in the transition matrix and eigenvalues near 1 are equal.

---

<sup>9</sup>For better approximation results, choose momenta  $p^{(k)1}, \dots, p^{(k)m}$  according to  $P$ . This results in  $m$  transitions  $q^{(k)} \rightarrow \hat{q}^{(k)1}, \dots, q^{(k)} \rightarrow \hat{q}^{(k)m}$ .

It follows from perturbation analysis [7] that the eigenvectors  $X_1, \dots, X_c$  corresponding to the cluster of eigenvalues near 1 are *almost constant on each meta-stable conformation*, i.e., if  $B_i$  and  $B_j$  belong to the same conformation, then  $X_k(B_i) \approx X_k(B_j)$  for  $k = 1, \dots, c$ . Furthermore, the  $c$ -tuple of eigenvector components associated with each  $B_i$ ,

$$B_i \mapsto (X_1(B_i), \dots, X_c(B_i)),$$

is sufficient to identify the conformations in the case of weak coupling [7]. Each conformation is the collection of sets  $B_i$  with almost identical  $c$ -tuple. Thus, using the eigenvectors  $X_1, \dots, X_c$  we have incorporated the dynamics by encoding the discretization sets  $B_1, \dots, B_d$  through  $c$ -tuples. The identification of conformations is reduced to clustering these  $c$ -tuples with respect to (geometrical) similarity. We have implemented an algorithm, which also copes with larger perturbations in the eigenvector components due to stronger coupling between the conformations. A detailed description of the algorithm is given in [7].

At the end of this section, we want to address the problem of how to choose the discretization sets  $B_1, \dots, B_d$ . On the one hand, since we seek out dynamical conformations as unions of the  $B_i$ , the partitioning should be as fine as possible in order to allow “arbitrary shaped” conformations. On the other hand, a fine partitioning requires many states and transitions to accurately determine the transition probabilities in (3). We adopt the following strategy: Since conformational transitions should correspond to changes in the essential degrees of freedom, we define the discretization sets only in terms of these essential coordinates (see Sec. 2.1). Furthermore, we take only those essential degrees of freedom into account whose distributions are far from being broad Gaussian shaped. The distributions are partitioned into their Gaussian-like parts and the  $B_i$  are defined as collection of states that fit into a certain combination of these subdivisions.

### 3 Results

The approaches to identify representative, structure and dynamics based conformations were applied to the triribonucleotide adenylyl(3'-5')cytidyl(3'-5')cytidin (r(ACC)) model system in vacuum (Fig. 4). It consists of  $N = 70$  atoms, whose physical representation is based on the GROMOS96 extended atom force field [29].

**Sampling of the canonical density.** The simulation data were generated by means of an ATHMC sampling of the canonical density at  $T = 300\text{K}$ . The subtrajectories of length 80fs (femtoseconds) were computed by means of the Verlet discretization with a stepsize of 2fs. For these parameters,

HMC simulations typically require thousands of iterations only to leave the neighborhood of the initial configuration. Application of ATHMC (with adaptive temperatures between 300K and 400K) circumvents the problem: one observes frequent transitions in the crucial torsion angles of the molecule (for details see [12]). The simulation was divided into 4 Markov chains, each starting with a different state chosen from a high temperature run at 500K, which allowed the molecule to move into different conformations. The sampling took about 12h on a workstation with MIPS R10.000 processor. It was terminated by a convergence indicator [16] associated with the potential energy and all 37 torsion angles after 32.000 steps, resulting in the sampling sequence  $q^{(1)}, \dots, q^{(S)}$ . We have found slower convergence for the torsion angles of the terminal ribose. Since the temperature can change during the ATHMC run, each configuration is connected with a reweighting factor with respect to the canonical ensemble at 300K.

**Representative conformations.** For Cartesian coordinates and torsion angles there are respectively five and four essential degrees of freedom. The transformation process for the torsion angles is exemplified in Fig. 1 and Fig. 2. Figure 1 (top, left) shows the circular deviations  $\rho$  of the transformed torsion angles in decreasing order of magnitude. Only the first four transformed torsion angles have relevant circular deviation *and* are far from being Gaussian shaped (see Fig. 2)<sup>10</sup>, while the remaining transformed torsion angles are Gaussian like. On the top right part of Fig. 1 the first non-essential transformed torsion angle, which is the fifth in the sequence, is shown. The graphics at the bottom part of Fig. 1 show the circular deviations of the original torsion angles (left) in decreasing order and the distribution of the fifth torsion angle (right) in sequence. Clearly non-Gaussian distributions show about 10 of the 37 torsion angles.

In order to identify representative conformations (R-conformations), we determine the maxima for each distribution of the essential torsion angles (see Fig. 2). These maxima have been grouped to  $3 \times 3 \times 2 \times 2 = 36$  combinations, each of them defining a theoretical, but not necessarily realized configuration of the molecule. From 15 maxima combinations with non-vanishing weight, we have selected two representative conformations to visualize characteristic differences (Fig. 4).

**Structure based conformations.** Since for the current structural cluster algorithm the computational effort grows quadratically with the number of configurations, we have performed the algorithm based on a subensemble of 1000 configurations out of the 32000 sampling configurations.<sup>11</sup>

---

<sup>10</sup>We scaled the transformed torsion angles such that the range is between  $-180$  and  $+180$ .

<sup>11</sup>This selection is realized randomly, taking the different statistical weights of the configurations into account. Using a subensemble one is always in danger of losing relevant

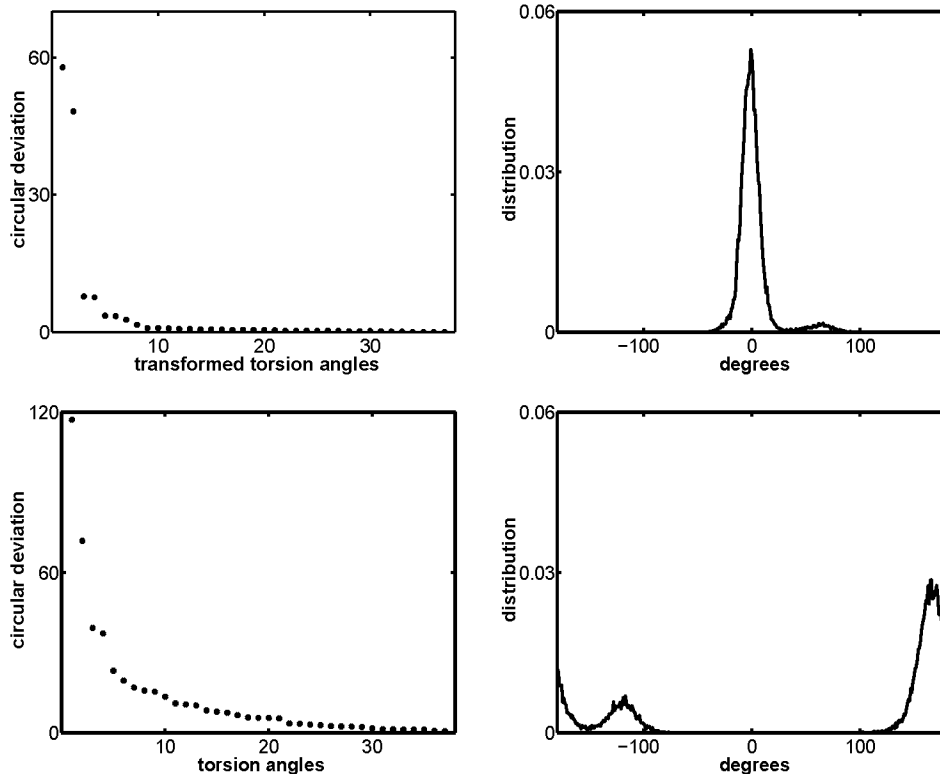


Figure 1: Top: circular deviation of the *transformed* torsion angles ordered by magnitude (left) and the distribution of the first non-essential torsion angle, which is the fifth angle in the sequence (right, see text). Bottom: circular deviation of the original torsion angles (left) and the distribution of the fifth torsion angle (right).

As stated in Section 2.2.1 the set of intra-molecular distances is overdetermined with respect to the number of degrees of freedom of a configuration. In order to emphasize differences between conformations and suppress smaller statistical vibrations, we reduce the set of intra-molecular distances to those with largest statistical variance in the sampling. To make sure that the reduced distance matrix still describes the whole molecule, we have selected  $3N$  pairs of atoms with largest variance such that each atom occurs information. Thus, it should be emphasized that the selection step is *not* necessary, i.e., one could also compute the required eigenvectors of the proximity matrix for the *entire* data set by applying subspace-oriented iterative eigenvalue solvers [6, 27]. However, in the case considered herein, the results to be presented do *not* depend sensitively on the length of the subensemble.

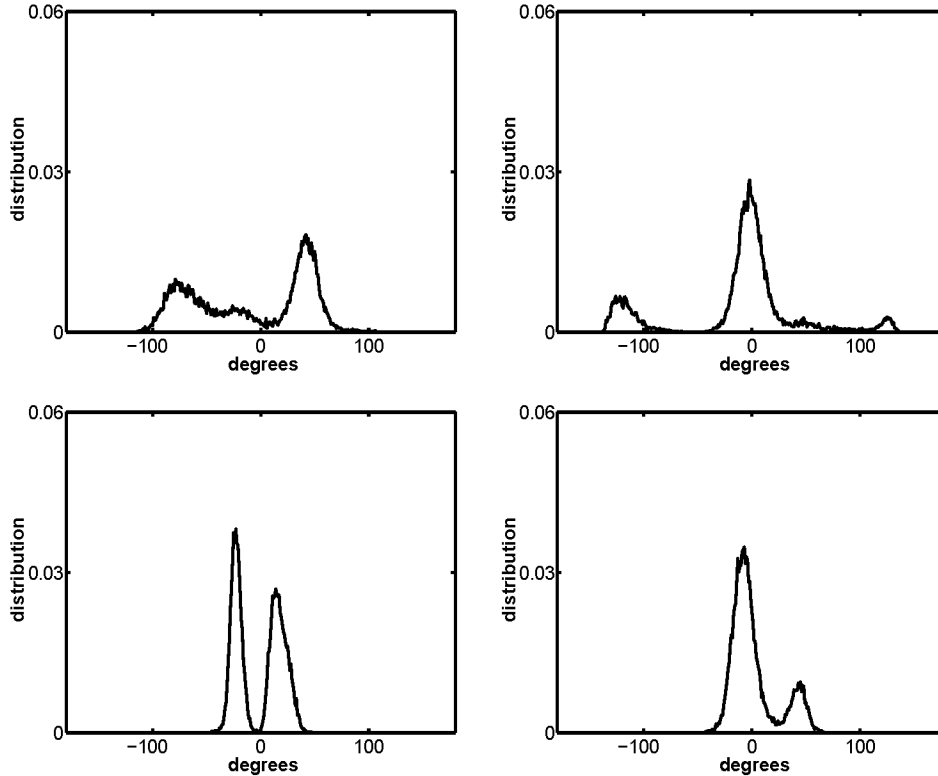


Figure 2: Distribution of the four essential torsion angles. The distributions at the top allow to identify three maxima each, while there are two maxima for each distribution at the bottom.

three times in the pairs.

The identification of clusters is performed hierarchically. Clusters are split into two subclusters according to the measure of similarity. During the process, many splits remove only a few data points from the parent cluster, i.e., the cluster from which the current cluster was split off, as our measure of proximity is inclined to do for combinatorial reasons. As a consequence, we consolidate the cluster hierarchy by removing all clusters that have fewer than ten data points. We characterize the clusters by the average distance of their members in comparison to the average distance of all data points or to the average distance in the father cluster. The latter measure indicates, in particular, good clustering properties.

We use a multidimensional scaling plot (Fig. 6 and Fig. 7) to visualize clusters [3]. The 2d-plot shows a 2d least squares approximation of the  $3N = 210$  dimensional configurational space in the sense that neighboring



points correspond in general to structurally similar configurations, while distant points reflect in general structural differences.

The structural clusters (S-clusters) are shown in Fig. 6. On the top level of hierarchy, there are three well separated clusters S1&S2, S3&S4 and S5, two of which can be split again giving a total of five clusters S1, . . . , S5. The structural clustering took less than 4% of the computing time required for evaluation of the simulation data.

**Dynamics based conformations.** The dynamical fluctuations within the canonical ensemble were approximated by integrating four short trajectories of length  $\tau = 80$ fs starting from each sampling point  $q^{(1)}, \dots, q^{(S)}$ . To facilitate transitions, analogous to the ATHMC sampling, the momenta were chosen according to the momenta distribution  $P(p)$  for 4 different temperatures between 300K – 400K and reweighted afterwards. This resulted in a total of  $4 \times 32.000 = 128.000$  transitions. This calculation took less than 25 % of the total computing time.

The configurational space was discretized into boxes  $B_1, \dots, B_d$ , by means of all four essential degrees of freedom (see Fig. 2) resulting in  $d = 36$  discretization boxes. Then the  $36 \times 36$  transition matrix  $P$  was computed based on the 128.000 transitions taking the different weighting factors into account. Since every box had been hit by sufficiently many transitions, the statistical sampling was accepted to be reliable. The computation of the eigenvalues of  $P$  near 1 yielded a cluster of eight eigenvalues with a significant gap to the remaining part of the spectrum:

$k$	1	2	3	4	5	6	7	8	9	...
$\lambda_k$	1.000	0.999	0.989	0.974	0.963	0.946	0.933	0.904	0.805	...

Finally, the dynamics based conformations (D-conformations) were computed based on the corresponding eight eigenvectors of  $P$  via the cluster algorithm presented in Section 2.2.2. We found eight D-conformations, which we have displayed in the multidimensional scaling plot based on structural proximity (Fig. 7). The clustering turned out to be rather insensitive to further refinements of the discretization. The weighting factors within the canonical ensemble and the meta-stability  $p_\tau(D, D)$  of the eight identified conformations are given in the following table:

conformations	D1c	D1t	D2c	D2t	D3c	D3t	D4c	D4t
weighting factor	0.107	0.011	0.116	0.028	0.320	0.038	0.285	0.095
meta-stability	0.986	0.938	0.961	0.888	0.991	0.949	0.981	0.962

The transition probabilities between the different D-conformations are visualized schematically in Fig. 3. In the limit of infinitely many transitions, the transition matrix should exploit a reversible, but not symmetric structure. Furthermore, the matrix allows to define a hierarchy between the clusters, which is inherent to the algorithm. On the top level, there are two

clusters, D1&D2 and D3&D4 corresponding to the two  $4 \times 4$  blocks on the diagonal. On the next level, each of these clusters split up into two subclusters yielding D1, ..., D4. On the bottom level, each cluster is further divided into a core (c) and a transition (t) part. The dynamical clustering took less than 2% of the computing time required for evaluation of the simulation data.

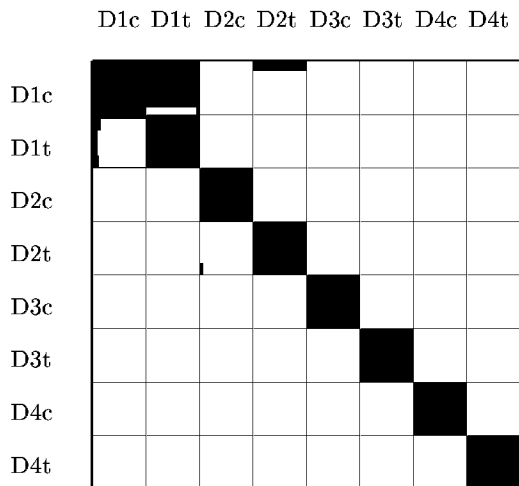


Figure 3: Schematical visualization of the transition probabilities  $p_\tau(D_{\text{from}}, D_{\text{to}})$  between the dynamical conformation  $D_{\text{from}}$  (row) and  $D_{\text{to}}$  (column). The colors are chosen according to the logarithm of the corresponding entries; black:  $p_\tau \approx 1$ , white:  $p_\tau \approx 0$ .

## 4 Discussion

Comparing dynamics and structure based conformations by means of Fig. 6 and Fig. 7 manifests the characteristics of each concept. The four conformations S1, ..., S4 correspond to D1, ..., D4, while S5 is part of all four dynamical conformations. This is made more precise by the following table, which shows the percentage of S-conformations in D-conformations:

	D1	D2	D3	D4
S1	1.000	0.000	0.000	0.000
S2	0.000	1.000	0.000	0.000
S3	0.000	0.000	0.994	0.006
S4	0.000	0.000	0.000	1.000
S5	0.121	0.697	0.015	0.167

The table indicates, that structural similarity and meta-stability might coincide. However, a difference between the two concepts is given by the last row. While S5 is composed of structurally similar configurations, it is by no means meta-stable, being spread out all over the four D-conformations. This might indicate that S5 is a collection of transition states, which do not cluster due to their similarity among each other, but rather due to their structural difference to all other states. In the dynamical analysis, these transition states are grouped to those clusters, to which they fluctuate most likely.

Fig. 4 shows two representative conformations with characteristic differences, selected out of the 15 representative conformations with non-vanishing weighting factor (see end of Sec. 2.1). Analyzing representative conformations in comparison to conformational ensembles, we have found, that the first six conformations with highest weights belong to the four dominant dynamical clusters D1, . . . ,D4. Of course, with the described method we will expect to find more representative conformations than dynamical clusters. The combination of maxima in the distribution of transformed torsion angles actually indicates a possible discretization of the state space into relatively few boxes. Each meta-stable conformational ensemble is composed of some of these boxes such that the number of conformational ensembles should be less than (or at most equal to) the number of representative conformations.

The conformations in Fig. 4 belong to the clusters D2 and D3 and can be visually distinguished according to the orientation of the  $\chi$  angle around the first glycosidic bond and the conformation of the terminal ribose, indicated by the so called sugar pucker  $P$ . In order to analyze, whether the two R-conformations allow to represent the two dynamical conformations, we plotted the distributions of the  $\chi$  and one of the torsion angles (within the sugar pucker  $P$ ) for the D2 and D3 conformation in comparison to all sampled states (Fig. 5). Obviously, the structural differences between the states in the conformational ensembles D2 and D3 can be described by differences in the ribose conformation and in the orientation of the adenine.

Torsion angle fluctuations at terminal groups have only minor influence on the global structure of the molecule. However, they may influence the covariance analysis based on torsion angles and thus the essential degrees of freedom. There are two possible remedies. On the one hand, one can switch to a representation in Cartesian coordinates, but then the overall translational and rotational motion of the molecule have to be eliminated. On the other hand, one can exclude all torsion angles corresponding to terminal groups for the covariance analysis. We favor the latter approach, since the chemical intuition and the imagination of global changes are facilitated in the space of torsion angles.

**Concluding remarks:** It is intriguing to apply “data mining”-oriented

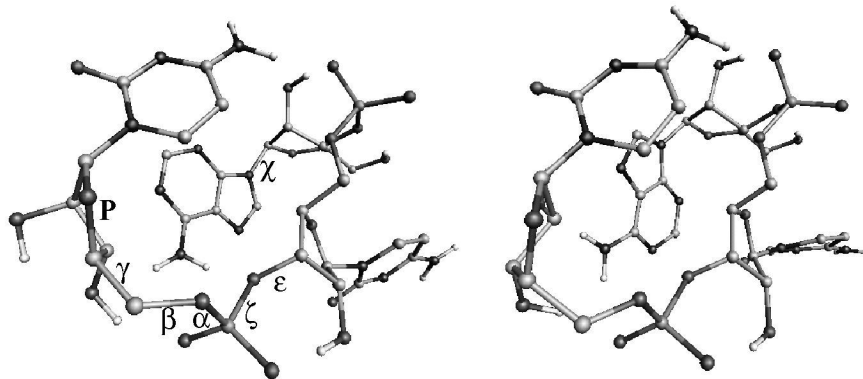


Figure 4: Two conformations of r(ACC). Left: The  $\chi$  angle around the first glycosidic bond is in *anti* position (-175. degrees) and the terminal ribose pucker  $P$  is in C(3')endo C(2')exo conformation. Right: The  $\chi$  angle is in *syn* position (19. degrees) and the terminal ribose in C(2')endo C(3')exo conformation.

statistical techniques to large data sets originating from MD or MC samplings of molecular ensembles. The idea of using cluster methods naturally leads to the concept of decomposing the data set into *conformational ensembles* or *subsets*, which can either be defined via their significant metastability or via structural similarities between the molecular configurations contained. This clustering of configurations into conformational ensembles is clearly different from the concept of choosing *single conformations* as representatives for common properties of a larger set of configurations. A few representative conformations allow a rough but fast examination of the state space, while the concept of conformational ensembles enables the investigation of structural conservation or meta-stability in the case of dynamical based methods. The latter approach can additionally be used to calculate transition rates between conformational ensembles and to locate transition states.

## References

- [1] Andrea Amadei, Antonius B. M. Linssen, and Herman J. C. Berendsen. Essential dynamics of proteins. *Proteins*, 17:412–425, 1993.
- [2] Michael R. Anderberg. *Cluster Analysis for Applications*. Academic Press, New York and London, 1973.
- [3] Christoph Best and Hans-Christian Hege. Visualizing conformations in molecular dynamics. Preprint SC 98-42, Konrad-Zuse-Zentrum für Informationstechnik Berlin (ZIB), 1998.

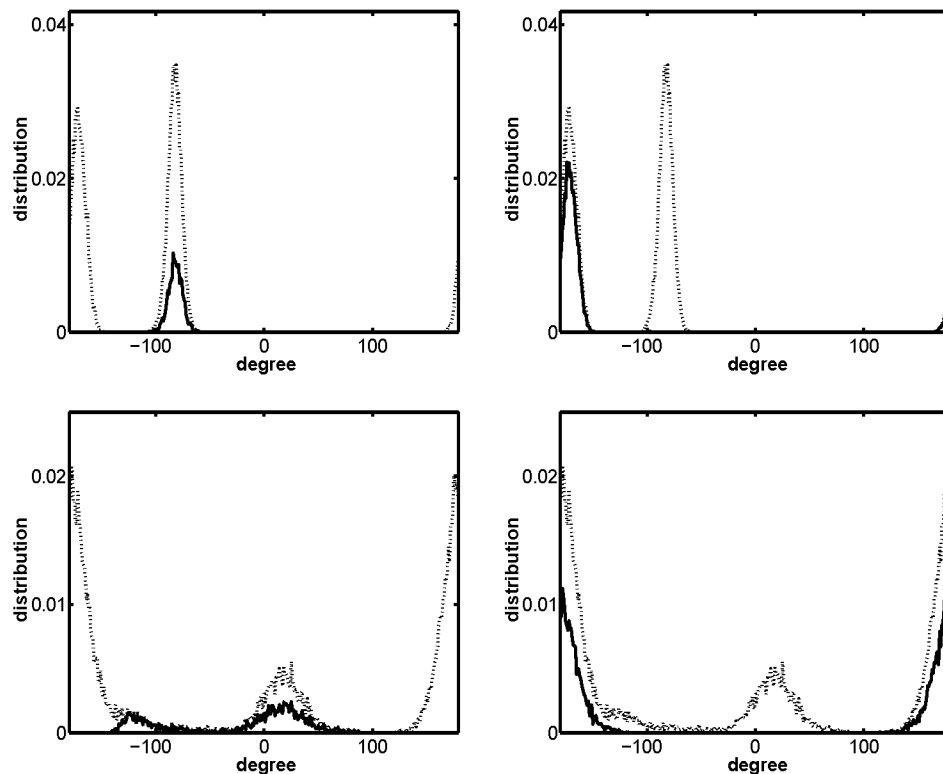


Figure 5: Distribution of torsion angles for all sampling data (dashed line) and selected clusters (solid line). Top: Distribution of one torsion angle at the terminal ribose for the conformations D2 (left) and D3 (right). Bottom: Distribution of the  $\chi$  angle (see Fig. 4) at the adenine for the conformations D2 (left) and D3 (right).

- [4] F. Cordes, E.B. Starikov, and W. Saenger. Initial state of an enzymatic reaction. Theoretical prediction of complex formation in the active site of RNase T1. *J. Am. Chem.Soc.*, 117:10365–10372, 1995.
- [5] X. Daura, B. Jaun, D. Seebach, W.F. van Gunsteren, and A.E. Mark. Reversible peptide folding in solution by molecular dynamics simulation. *J. Mol. Biol.*, 280:925–932, 1998.
- [6] P. Deuffhard, T. Friese, and F. Schmidt. A nonlinear multigrid eigenproblem solver for the complex Helmholtz equation. Konrad-Zuse-Zentrum Berlin, Preprint SC 97-55, 1997.
- [7] P. Deuffhard, W. Huisinga, A. Fischer, and Ch. Schütte. Identification of almost invariant aggregates in nearly uncoupled Markov chains. Preprint SC-98-03, Konrad-Zuse-Zentrum, Berlin. Available via <http://www.zib.de/huisinga>, 1998.
- [8] P. Drineas, A. Frieze, R. Kannan, S. Vempala, and V. Vinay. Clustering in large graphs and matrices. Preprint, Yale University, Dept. of Computer Science, to appear

- in the Proceedings of the Symposium on Discrete Algorithms, SIAM, 1999.
- [9] Y. Duan and P.A. Kollman. Pathways to a protein folding intermediate observed in a 1-microsecond simulation in aqueous solution. *Science*, 282:740–744, 1998.
  - [10] Miroslav Fiedler. Eigenvectors of acyclic matrices. *Czech. Math. J.* 25(100), pages 607–618, 1975.
  - [11] Miroslav Fiedler. A property of eigenvectors of nonnegative symmetric matrices and its application to graph theory. *Czech. Math. J.* 25(100), pages 619–633, 1975.
  - [12] A. Fischer, F. Cordes, and Ch. Schütte. Hybrid Monte Carlo with adaptive temperature in mixed-canonical ensemble: Efficient conformational analysis of RNA. *J. Comput. Chem.*, 19:1689–1697, 1998.
  - [13] Nick I. Fisher. *Statistical analysis of circular data*. Cambridge University Press, 1993.
  - [14] Nick I. Fisher and A. J. Lee. A correlation coefficient for circular data. *Biometrika*, 70(2):327–332, 1983.
  - [15] H. Frauenfelder, S.G. Sligar, and P.G. Wolynes. The energy landscapes and motions of proteins. *Science*, 254:1598–1603, 1991.
  - [16] A. Gelman and D.B. Rubin. Inference from iterative simulation using multiple sequences. *Statistical Science*, 7:457–511, 1992.
  - [17] M. Gerstein, A.M. Lesk, and C. Clothia. Structural mechanisms for domain movements in proteins. *Biochemistry*, 33:6739–6749, 1994.
  - [18] H.L. Gordon and R.L. Somorjai. Fuzzy cluster analysis for molecular dynamics trajectories. *Proteins*, 14:249–264, 1992.
  - [19] H. Grubmüller, B. Heymann, and P. Tavan. Molecular mechanics calculation of the streptavidin-biotin rupture force. *Science*, 271:997–999, 1996.
  - [20] S. Hayward and H.J.C. Berendsen. Systematic analysis of domain movements in proteins from conformational change: New results on citrate synthase and T4 lysozyme. *Proteins*, 30:144–154, 1998.
  - [21] S. Hayward, A. Kitao, and H.B.C. Berendsen. Model-free methods of analyzing domain motions in proteins from simulation: A comparison of normal mode analysis and molecular dynamic simulation of lysozyme. *Proteins*, 27:425–437, 1997.
  - [22] Bruce Hendrickson and Robert Leland. An improved spectral graph partitioning algorithm for mapping parallel computations. *SIAM J. Sci. Comput.* 16(2), pages 452–469, 1995.
  - [23] Anil K. Jain and Richard C. Dubes. *Algorithms for Clustering Data*. Prentice Hall, Advanced Reference Series edition, 1988.
  - [24] P. E. Jupp and K. V. Mardia. A unified view of the theory of directional statistics, 1975–1988. *Int. Statist. Rev.*, 57(3):261–294, 1989.
  - [25] M.E. Karpen, D.J. Tobias, and C.L. Brooks III. Statistical clustering techniques for the analysis of long molecular dynamics trajectories: Analysis of 2.2-ns trajectories of YPGDV. *Biochemistry*, 32:412–420, 1993.
  - [26] Martin Kloppenburg and Paul Tavan. Deterministic annealing for density estimation by multivariate normal mixtures. *Phys. Rev. E*, 55(3-A), 1997.
  - [27] R. B. Lehoucq, D. C. Sorensen, and C. Yang. *ARPACK User's Guide: Solution of Large Eigenvalue Problems by Implicit Restarted Arnoldi Methods*. Rice University Houston, 1998.
  - [28] Ch. Schütte, A. Fischer, W. Huisinga, and P. Deuffhard. A direct approach to conformational dynamics based on hybrid Monte Carlo. Preprint SC-98-45, Konrad-Zuse-Zentrum, Berlin. Available via <http://www.zib.de/bib/pub/pw/>, 1998.

- [29] W. F. van Gunsteren, S. R. Billeter, A. A. Eising, P. H. Hünenberger, P. Krüger, A. E. Mark, W. R. P. Scott, and I. G. Tironi. *Biomolecular Simulation: The GROMOS96 Manual and User Guide*. vdf Hochschulverlag AG, ETH Zürich, 1996.
- [30] H.X. Zhou, S.T. Wlodek, and J.A. McCammon. Conformation gating as a mechanism for enzyme specificity. *Proc. Nat. Acad. Sci.*, 95:9280–9283, 1998.

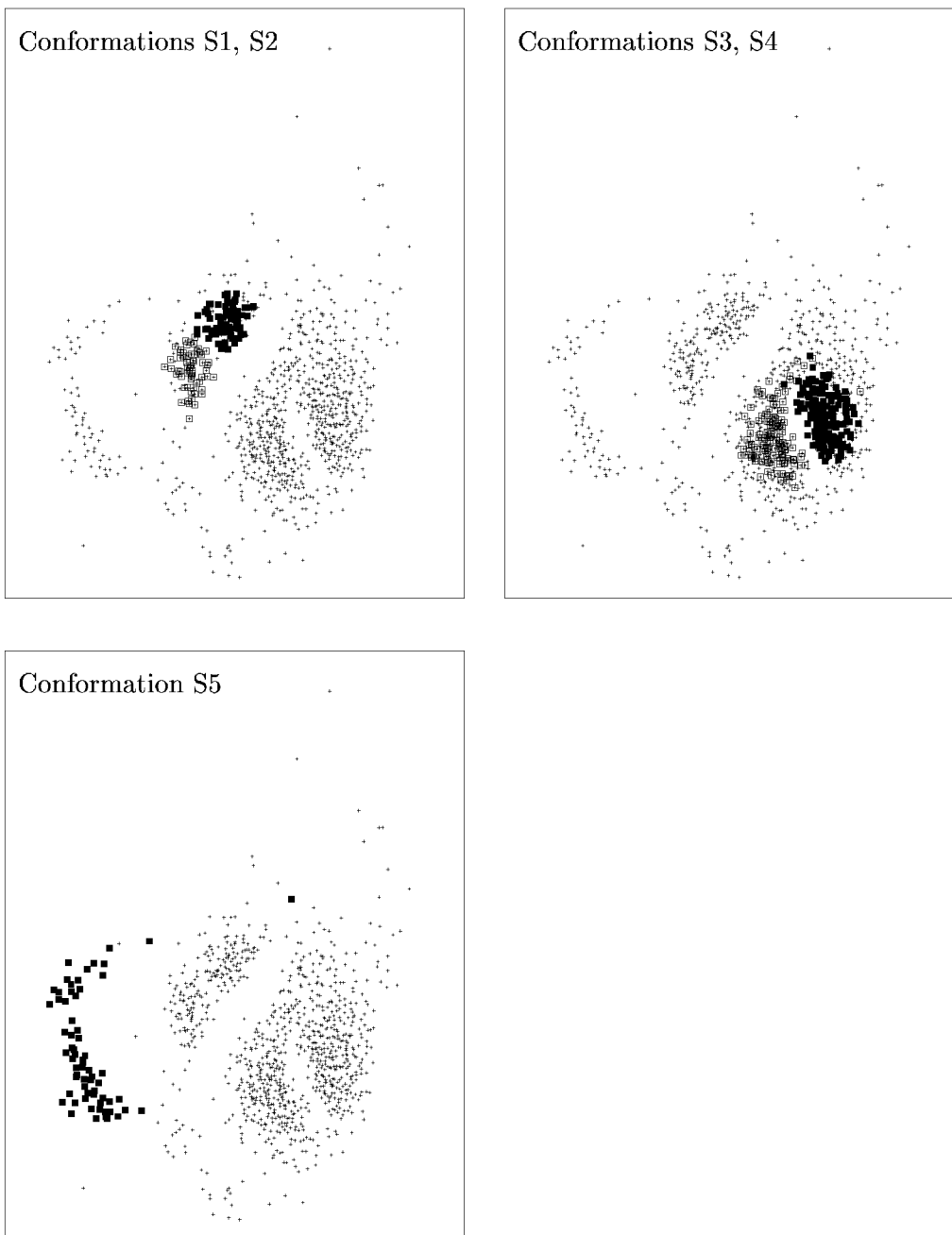


Figure 6: 2d plot of the five structure based conformations  $S_1, \dots, S_5$ . The distinction between open and filled squares indicates a the splitting into subsets.



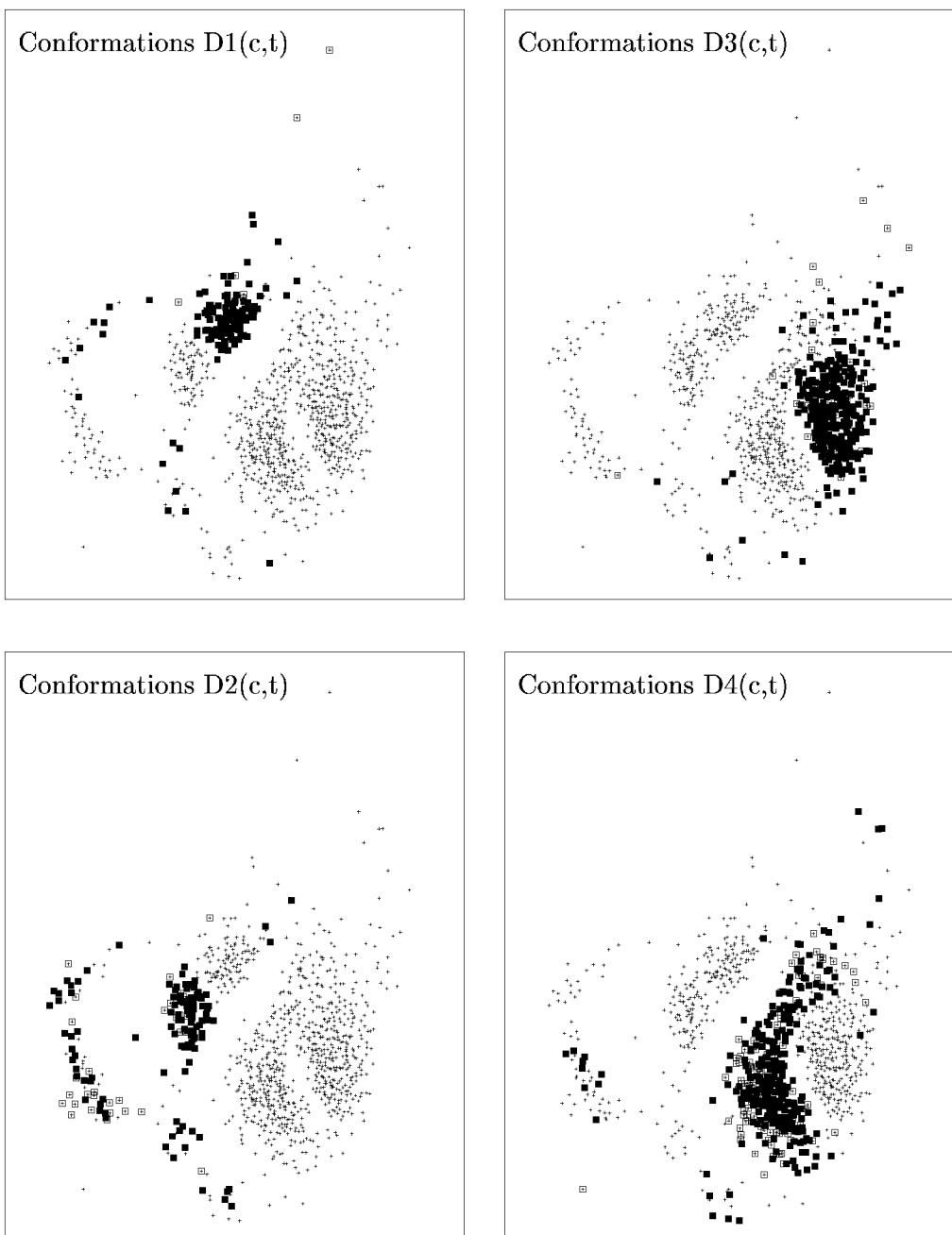


Figure 7: 2d plot of the four dynamical conformations  $D1, \dots, D4$  (squares). The distinction between open and filled squares indicates a further splitting into eight conformations resulting from a partition into a core( $c$ ) and a transition( $t$ ) conformation.